Multi-Channel ECG and Noise Modeling: Application to Maternal and Fetal ECG Signals

Reza Sameni[1,2], Gari D. Clifford[3], Christian Jutten[2], Mohammad B. Shamsollahi[1]
1- School of Electrical Engineering, Sharif University of Technology, Tehran, Iran
2- Laboratoire des Images et des Signaux (LIS) – CNRS UMR 5083, INPG, UJF, Grenoble, France
3- Laboratory for Computational Physiology, Harvard-MIT Division of Health Sciences and Technology (HST), Cambridge MA, USA
Emails: reza.sameni@lis.inpg.fr, gari@mit.edu, christian.jutten@lis.inpg.fr, mbshams@sharif.ir
Address: Laboratoire des Images et des Signaux (LIS), 46 Avenue Félix Viallet, 38031 Grenoble Cedex, France
Phone: +33(0)476574355 - Fax: +33(0)4765747

***Abstract*— In this paper, a three dimensional dynamic model of the electrical activity of the heart is presented. The model is based on the single dipole model of the heart and is later related to the body surface potentials through a linear model which accounts for the temporal movements and rotations of the cardiac dipole, together with a realistic ECG noise model. The proposed model is also generalized to maternal and fetal ECG mixtures recorded from the abdomen of pregnant women in single and multiple pregnancies. The applicability of the model for the evaluation of signal processing algorithms is illustrated using Independent Component Analysis. Considering the difficulties and limitations of recording long-term ECG data, especially from pregnant women, the model described in this article may serve as an effective means of simulation and analysis of a wide range of ECGs, including adults and fetuses.**

I. Introduction

The electrical activity of the cardiac muscle and its relationship with the body surface potentials, namely the *Electrocardiogram* (ECG), has been studied with different approaches ranging from *single dipole models* to *activation maps* [1]. The goal of these models is to represent the cardiac activity in the simplest and most informative way for specific applications. However, depending on the application of interest, any of the proposed models have some level of abstraction, which makes them a compromise between simplicity, accuracy, and interpretability for cardiologists. Specifically, it is known that, the single dipole model and its variants [1], are equivalent source descriptions of the true cardiac potentials. This means that they can only be used as far-field approximations of the cardiac activity, and do not have evident interpretations in terms of the underlying electrophysiology [2]. However, despite these intrinsic limitations, the single dipole model still remains a popular model, since it accounts for 80% to 90% of the power of the body surface potentials [2], [3].

Statistical decomposition techniques such as *Principal Component Analysis* (PCA) [4], [5], [6], [7], and more recently *Independent Component Analysis* (ICA) [6], [8], [9], [10] have been widely used as promising methods of multi-channel ECG analysis, and noninvasive fetal ECG extraction. However, there are many issues such as the interpretation, stability, robustness, and noise-sensitivity of the extracted components. These issues are left as open problems and require further studies by using realistic models of these signals [11]. Note that, most of these algorithms have been applied *blindly*, meaning that the *a priori* information about the underlying signal sources and the propagation media have not been considered. This suggests that by using additional information such as the temporal dynamics of the cardiac signal (even through approximate models such as the single dipole model), we can improve the performance of existing signal processing methods. Examples of such improvements have been previously reported in other contexts ([12] chapters 11 and 12).

In recent years research has been conducted towards the generation of synthetic ECG signals to facilitate the testing of signal processing algorithms. Specifically, in [13], [14] a dynamic model has been developed, which reproduces the morphology of the PQRST complex and their relationship to the beat-to-beat (RR-interval) timing in a single nonlinear dynamic model. Considering the simplicity and flexibility of this model it is reasonable to assume that it can be easily adapted to a broad class of normal and abnormal ECGs. However previous works are restricted to single channel ECG modeling, meaning that the parameters of the model should be re-calculated for each of the recording channels. Moreover, for the maternal and fetal mixtures recorded from the abdomen of pregnant women, there are very few works which have both considered the cardiac source and the propagation media [4], [15], [16].

Real ECG recordings are always contaminated with noise and artifacts; hence besides the modeling of the cardiac sources and the propagation media, it is very important to have realistic models for the noise sources. Since common ECG contaminants are non-stationary and temporally correlated, time-varying dynamic models are required for the generation of realistic noises.

In the following, a three dimensional canonical model of the single dipole vector of the heart is proposed. This model, which is inspired by the single-channel ECG dynamic model presented in [13], is later related to the body surface potentials through a linear model that accounts for the temporal movements and rotations of the cardiac dipole, together with a model for the generation of realistic ECG noise. The ECG model is then generalized to fetal ECG signals recorded from the maternal abdomen. The model described in this article is believed to be an effective means of providing realistic simulations of maternal/fetal ECG mixtures in single and

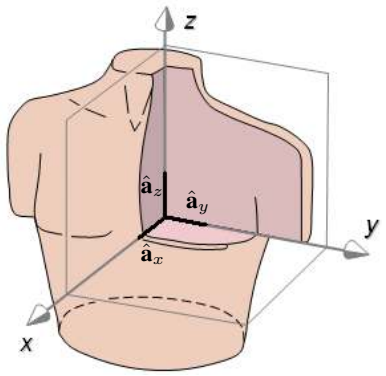

Fig. 1. The three body axes. Adapted from [3].

multiple pregnancies.

II. The Cardiac Dipole vs. the Electrocardiogram

According to the single dipole model of the heart, the myocardium's electrical activity may be represented by a time-varying rotating vector, the origin of which is assumed to be at the center of the heart as its end sweeps out a quasi-periodic path through the torso. This vector may be mathematically represented in the Cartesian coordinates, as follows:

$$\mathbf{d}(t) = x(t)\hat{\mathbf{a}}_x + y(t)\hat{\mathbf{a}}_y + z(t)\hat{\mathbf{a}}_z, \tag{1}$$

where $\hat{\mathbf{a}}_x$, $\hat{\mathbf{a}}_y$, and $\hat{\mathbf{a}}_z$ are the unit vectors of the three body axes shown in Fig. 1. With this definition, and by assuming the body *volume conductor* as a passive resistive medium which only attenuates the source field [17], any ECG signal recorded from the body surface would be a linear projection of the dipole vector $\mathbf{d}(t)$, onto the direction of the recording electrode axes $\mathbf{v} = a\hat{\mathbf{a}}_x + b\hat{\mathbf{a}}_y + c\hat{\mathbf{a}}_z$:

$$ECG(t) =< \mathbf{d}(t), \mathbf{v} >= a \cdot x(t) + b \cdot y(t) + c \cdot z(t) \tag{2}$$

As a simplified example, consider the dipole source of $\mathbf{d}(t)$ inside a homogeneous infinite volume conductor. The potential generated by this dipole at a distance of $|\mathbf{r}|$ is:

$$\phi(t) - \phi_0 = \frac{\mathbf{d}(t)\cdot\mathbf{r}}{4\pi\sigma|\mathbf{r}|^3} = \frac{1}{4\pi\sigma}[x(t)\frac{r_x}{|\mathbf{r}|^3} + y(t)\frac{r_y}{|\mathbf{r}|^3} + z(t)\frac{r_z}{|\mathbf{r}|^3}] \tag{3}$$

where ϕ_0 is the reference potential, $\mathbf{r} = r_x\hat{\mathbf{a}}_x + r_y\hat{\mathbf{a}}_y + r_z\hat{\mathbf{a}}_z$ is the vector which connects the center of the dipole to the observation point, and σ is the conductivity of the volume conductor [3], [17]. Now consider the fact that the ECG signals recorded from the body surface are the potential differences between two different points. Equation (3) therefore indicates how the coefficients a, b, and c in (2) can be related to the radial distance of the electrodes and the volume conductor material. Of course, in reality the volume conductor is neither homogeneous nor infinite, leading to a much more complex relationship between the dipole source and the body surface potentials. However even with a complete volume conductor model, the body surface potentials are linear instantaneous mixtures of the cardiac potentials [17].

A 3-dimensional vector representation of the ECG, namely the *Vectorcardiogram* (VCG), is also possible by using three of such ECG signals. Basically any set of three linearly independent ECG electrode leads can be used to construct the VCG. However, in order to achieve an orthonormal representation that best resembles the dipole vector $\mathbf{d}(t)$, a set of three orthogonal leads that correspond with the three body axes are selected. The normality of the representation is further achieved by attenuating the different leads with *a priori* knowledge of the body volume conductor, to compensate for the non-homogeneity of the body thorax [3]. The *Frank lead system* [18], or the *corrected Frank lead system* [19] which has better orthogonality and normalization, are conventional methods for recording the VCG.

Based on the single dipole model of the heart, Dower *et al* have developed a transformation for finding the standard 12-lead ECGs from the Frank electrodes [20]. The Dower transform is simply a 12×3 linear transformation between the standard 12-lead ECGs and the Frank leads, which can be found from the *Minimum Mean Square Error* (MMSE) estimate of a transformation matrix between the two electrode sets. Apparently the transformation is influenced by the standard locations of the recording leads and the attenuations of the body volume conductor, with respect to each electrode [21]. The Dower transform and its inverse [22], are evident results of the single dipole model of the heart with a linear propagation model of the body volume conductor. However, since the single dipole model of the heart is not a perfect representation of the cardiac activity, cardiologists usually use more than three ECG electrodes (between six to twelve) to study the cardiac activity [3].

III. Heart dipole vector and ECG modeling

Different ECG leads can be assumed to be projections of the heart's dipole vector onto the recording electrode axes. All leads are therefore time synchronized with each other and have a quasi-periodic shape. Based on the single channel ECG model proposed in [13] (and later updated in [23], [24], and [25]), the following dynamic model is suggested for the $\mathbf{d}(t)$ dipole vector:

$$\begin{aligned}
\dot{\theta} &= \omega \\
\dot{x} &= -\sum_i \frac{\alpha_i^x \omega}{(b_i^x)^2}\Delta\theta_i^x exp[-\frac{(\Delta\theta_i^x)^2}{2(b_i^x)^2}] \\
\dot{y} &= -\sum_i \frac{\alpha_i^y \omega}{(b_i^y)^2}\Delta\theta_i^y exp[-\frac{(\Delta\theta_i^y)^2}{2(b_i^y)^2}] \\
\dot{z} &= -\sum_i \frac{\alpha_i^z \omega}{(b_i^z)^2}\Delta\theta_i^z exp[-\frac{(\Delta\theta_i^z)^2}{2(b_i^z)^2}]
\end{aligned} \tag{4}$$

where $\Delta\theta_i^x = (\theta - \theta_i^x) mod(2\pi)$, $\Delta\theta_i^y = (\theta - \theta_i^y) mod(2\pi)$, $\Delta\theta_i^z = (\theta - \theta_i^z) mod(2\pi)$, and $\omega = 2\pi f$, where f is the beat-to-beat heart rate. Accordingly, the first equation in (4) generates a circular trajectory rotating with the frequency of the heart rate. Each of the three coordinates of the dipole vector $\mathbf{d}(t)$, is modeled by a summation of Gaussian functions with the amplitudes of α_i^x, α_i^y, and α_i^z; widths of b_i^x, b_i^y, and b_i^z; and located at the rotational angles of θ_i^x, θ_i^y, and θ_i^z. The intuition behind this set of equations is, that the

baseline of each of the dipole coordinates is pushed up and down, as the trajectory approaches the centers of the Gaussian functions, generating a moving and variable length vector in the (x, y, z) space. Moreover, by adding some deviations to the parameters of (4) (i.e. considering them as random variables rather than deterministic constants), it is possible to generate more realistic cardiac dipoles with inter-beat variations.

This model of the rotating dipole vector is rather general, since due to the *universal approximation* property of Gaussian mixtures, any continuous function (as the dipole vector is assumed to be so), can be modeled with a sufficient number of Gaussian functions up-to an arbitrarily close approximation [26].

Equation (4) can also be thought as a model for the orthogonal lead VCG coordinates, with an appropriate scaling factor for the attenuations of the volume conductor. This analogy between the orthogonal VCG and the dipole vector can be used to estimate the parameters of (4) from the three Frank lead VCG recordings. As an illustration typical signals recorded from the Frank leads and the dipole vector modeled by (4) are plotted in Figs. 2 and 3. The parameters of (4), used for the generation of these figures are presented in Table I. These parameters have been estimated from the best MMSE fitting between N Gaussian functions and the Frank lead signals. As it can be seen in Table I, the number of the Gaussian functions are not necessarily the same for the different channels, and can be selected according to the shape of the desired channel.

A. Multi-channel ECG modeling

The dynamic model in (4) is a representation of the dipole vector of the heart (or equivalently the orthogonal VCG recordings). In order to relate this model to realistic multi-channel ECG signals recorded from the body surface, we need an additional model to project the dipole vector onto the body surface by considering the propagation of the signals in the body volume conductor, the possible rotations and scalings of the dipole, and the ECG measurement noises. Following the discussions of section II, a rather simplified linear model which accounts for these measures and is in accordance with (2) and (3) is suggested as follows:

$$ECG(t) = H \cdot R \cdot \Lambda \cdot s(t) + W(t) \tag{5}$$

where $ECG(t)_{N\times 1}$ is a vector of the ECG channels recorded from N leads, $s(t)_{3\times 1} = [x(t), y(t), z(t)]^T$ contains the three components of the dipole vector $\mathbf{d}(t)$, $H_{N\times 3}$ corresponds to the body volume conductor model (as for the Dower transformation matrix), $\Lambda_{3\times 3} = diag(\lambda_x, \lambda_y, \lambda_z)$ is a diagonal matrix corresponding to the scaling of the dipole in each of the x, y, and z directions, $R_{3\times 3}$ is the rotation matrix for the dipole vector, and $W(t)_{N\times 1}$ is the noise in each of the N ECG channels at the time instance of t. Note that H, R, and Λ matrices are generally functions of time.

Although the product of $H \cdot R \cdot \Lambda$ may be assumed to be a single matrix, the representation in (5) has the benefit that the rather stationary features of the body volume conductor that depend on the location of the ECG electrodes and the conductivity of the body tissues can be considered in H, while the temporal inter-beat movements of the heart can be considered in Λ and R, meaning that their average values are identity matrices in a long term study: $E_t\{R\} = I$, $E_t\{\Lambda\} = I$. In Appendix I by using the Givens rotation, a means of coupling these matrices with external sources such as the respiration and achieving non-stationary mixtures of the dipole source is presented.

B. Modeling maternal abdominal recordings

By utilizing a dynamic model like (4) for the dipole vector of the heart, the signals recorded from the abdomen of a pregnant woman, containing the fetal and maternal heart components can be modeled as follows:

$$X(t) = H_m \cdot R_m \cdot \Lambda_m \cdot s_m(t) + H_f \cdot R_f \cdot \Lambda_f \cdot s_f(t) + W(t) \tag{6}$$

where the matrices H_m, H_f, R_m, R_f, Λ_m and, Λ_f have similar definitions as the ones in (5), with the subscripts of m and f referring to the mother and the fetus, respectively. Moreover, R_f has the additional interpretation that its mean value ($E_t\{R_f\} = R_0$) is not an identity matrix and can be assumed as the relative position of the fetus with respect to the axes of the maternal body. This is an interesting feature

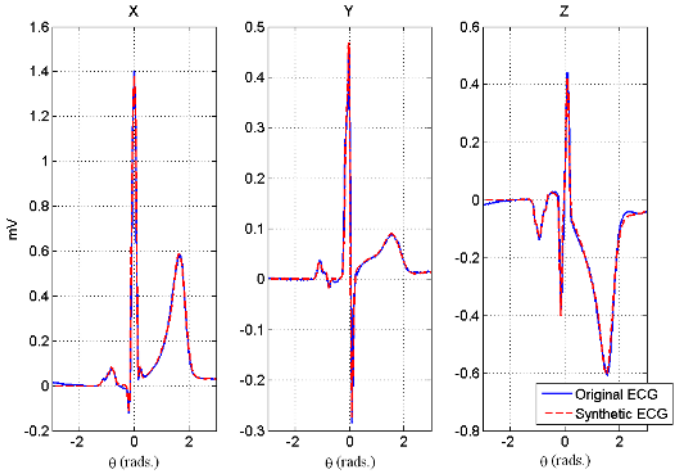

Fig. 2. Synthetic ECG signals of the Frank lead electrodes

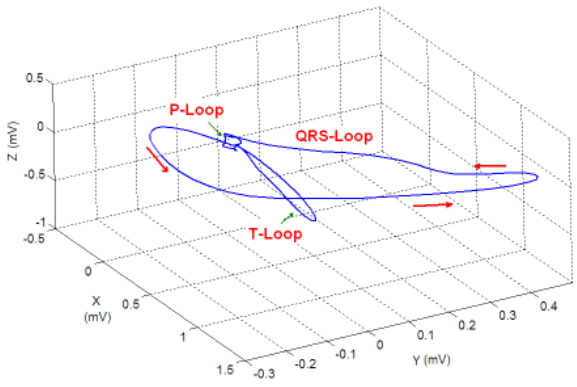

Fig. 3. Typical synthetic VCG loop. Arrows indicate the direction of rotation. Each clinical lead is produced by mapping this trajectory onto a 1-D vector in this 3-dimensional space.

TABLE I

PARAMETERS OF THE SYNTHETIC MODEL PRESENTED IN (4) FOR THE ECGS AND VCG PLOTTED IN FIGS. 2, 3

Index(i)	1	2	3	4	5	6	7	8	9	10	11
α_i^x(mV)	0.03	0.08	-0.13	0.85	1.11	0.75	0.06	0.10	0.17	0.39	0.03
b_i^x(rads.)	0.09	0.11	0.05	0.04	0.03	0.03	0.04	0.60	0.30	0.18	0.50
θ_i(rads.)	-1.09	-0.83	-0.19	-0.07	0.00	0.06	0.22	1.20	1.42	1.68	2.90
α_i^y(mV)	0.04	0.02	-0.02	0.32	0.51	-0.32	0.04	0.08	0.01		
b_i^y(rads.)	0.07	0.07	0.04	0.06	0.04	0.06	0.45	0.30	0.50	–	–
θ_j(rads.)	-1.10	-0.90	-0.76	-0.11	-0.01	0.07	0.80	1.58	2.90		
α_i^z(mV)	-0.03	-0.14	-0.04	0.05	-0.40	0.46	-0.12	-0.20	-0.35	-0.04	
b_i^z(rads.)	0.03	0.12	0.04	0.40	0.05	0.05	0.80	0.40	0.20	0.40	–
θ_k(rads.)	-1.10	-0.93	-0.70	-0.40	-0.15	0.10	1.05	1.25	1.55	2.80	

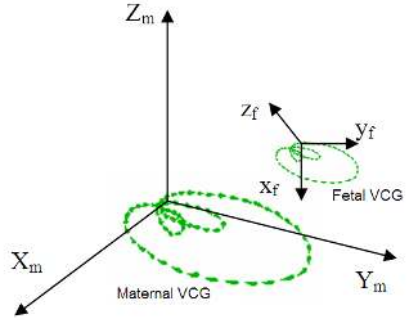

Fig. 4. Illustration of the fetal and maternal VCGs vs. their body coordinates

for modeling the fetus in the different typical positions such as *Vertex* (fetal head-down) or *Breech* (fetal head-up) positions [27]. As illustrated in Fig. 4, $s_f(t) = [x_f(t), y_f(t), z_f(t)]^T$ can be assumed as a canonical representation of the fetal dipole vector which is defined with respect to the fetal body axes, and in order to calculate this vector with respect to the maternal body axes, $s_f(t)$ should be rotated by the 3-dimensional rotation matrix of R_0:

$$R_0 = \begin{bmatrix} 1 & 0 & 0 \\ 0 & cos\theta_x & sin\theta_x \\ 0 & -sin\theta_x & cos\theta_x \end{bmatrix} \begin{bmatrix} cos\theta_y & 0 & sin\theta_y \\ 0 & 1 & 0 \\ -sin\theta_y & 0 & cos\theta_y \end{bmatrix} \times \begin{bmatrix} cos\theta_z & sin\theta_z & 0 \\ -sin\theta_z & cos\theta_z & 0 \\ 0 & 0 & 1 \end{bmatrix}, \tag{7}$$

where θ_x, θ_y, and θ_z are the angles of the fetal body planes with respect to the maternal body planes.

The model presented in (6) may be simply extended to multiple pregnancies (twins, triplets, quadruplets, etc.), by considering additional dynamic models for the other fetuses.

C. Fitting the model parameter to real recordings

As previously stated, due to the analogy between the dipole vector and the orthogonal lead VCG recordings, the number and shape of the Gaussian functions used in (4) can be estimated from typical VCG recordings. This estimation requires a set of orthogonal leads, such as the Frank leads, in order to calibrate the parameters. There are different possible approaches for the estimation of the Gaussian function parameters of each lead. *Nonlinear Least Square Error* (NLSE) methods, as previously suggested in [25], [28] have been proved as an effective approach. Otherwise, one can use the A^* optimization approach adopted in [26], or benefit from the algorithms developed for *Radial Basis Functions* (RBF) in the *Neural Network* context [29]. For the results of this paper, the NLSE approach has been used.

It should be noted that (4) is some kind of canonical representation of the heart's dipole vector; meaning that the amplitudes of the Gaussian terms in (4) are not the same as the ones recorded from the body surface. In fact, using (4) and (5) to generate synthetic ECG signals, there is an intrinsic indeterminacy between the scales of the entries of $s(t)$ and the mixing matrix H, since there is no way to record the true dipole vectors noninvasively. To solve this ambiguity, and without the loss of generality, it is suggested that we simply assume the dipole vector to have specific amplitudes, based on *a priori* knowledge of the VCG shape in each of its three coordinates, using realistic body torso models [30].

As mentioned before the H mixing matrix in (5) depends on the location of the recording electrodes. So in order to estimate this matrix, we first calculate the optimal parameters of (4) from the Frank leads of a given database. Next the H matrix is estimated by using a MMSE estimate between the synthetic dipole vector and the recorded ECG channels of the database. In fact by using the previously mentioned assumption that: $E_t\{R\} = I$ and $E_t\{\Lambda\} = I$, the MMSE solution of the problem is:

$$\hat{H} = E\{ECG(t) \cdot s(t)^T\}[E\{s(t) \cdot s(t)^T\}]^{-1} \tag{8}$$

For the case of abdominal recordings the estimation of the H_m and H_f matrices in (6) are more difficult and require *a priori* information about the location of the electrodes and a model for the propagation of the maternal and fetal signals within the maternal thorax and abdomen [16]. However, a coarse estimation of H_m can be achieved for a given configuration of abdominal electrodes by using (8) between the abdominal ECG recordings and three orthogonal leads placed close to the mother's heart for recording her VCG. Yet the accurate estimation of H_f requires more information about the maternal body, and more accurate non-homogeneous models of the volume conductor [4].

The ω term introduced in (4) is in general a time-variant parameter which depends on physiological factors such as the speed of electrical wave propagation in the cardiac muscle or the *heart rate variability* (HRV) [13]. Furthermore, since the phase of the respiratory cycle can be derived from the ECG (or through other means such as amplifying the differential change

in impedance in the thorax; impedance pneumography) and Λ is likely to vary with respiration, it is logical that an estimation of Λ over time can be made from such measurements.

The relative average (static) orientation of the fetal heart with respect to the maternal cardiac source is represented by R_0 which could be initially determined through a sonogram, and later inferred by referencing the signal to a large database of similar-term fetuses. Of course, both Λ and R_0 are functions of the respiration and heart rates and therefore tracking procedures such as *Expectation Maximization* (EM) [31], or *Kalman Filter* (KF) may be required for online adaptation of these parameters [24], [32].

IV. ECG Noise Modeling

An important issue that should be considered in the modeling of realistic ECG signals is to model realistic noise sources. Following [33], the most common high-amplitude ECG noises that cannot be removed by simple in-band filtering, are:

- Baseline Wander (BW)
- Muscle Artifact (MA)
- Electrode Movement (EM)

For the fetal ECG signals recorded from the maternal abdomen the following may also be added to this list:

- Maternal ECG
- Fetal movements
- Maternal uterus contractions
- Changes in the conductivity of the maternal volume conductor due to the development of the *vernix caseosa* layer around the fetus [4]

These noises are typically very non-stationary in time and colored in spectrum (having long-term correlations). This means that white noise or stationary colored noise, are generally insufficient to model ECG noise. In practice, researchers have preferred to use real ECG noises such as those found in the MIT-BIH *Non-Stress Test Database* (NSTDB) [34], [35], with varying Signal-to-Noise Ratios (SNRs). However, as explained in the following, parametric models such as time-varying *Autoregressive* (AR) models can be used to generate realistic ECG noises which follow the non-stationarity and the spectral shape of real noise. The parameters of this model can be trained by using real noises such as the NSTDB. Having trained the model, it can be driven by white noise to generate different instances of such noises, with almost identical temporal and spectral characteristics.

There are different approaches for the estimation of time-varying AR parameters. An efficient approach that was employed in this work, is to reformulate the AR model estimation problem in the form of a standard KF [36]. In a recent work, a similar approach has been effectively used for the time-varying analysis of the HRV [37].

For the time series of y_n, a time-varying AR model of order p can be described as follows:

$$\begin{aligned} y_n &= -a_{n1}y_{n-1} - a_{n2}y_{n-2} - ... - a_{np}y_{n-p} + v_n \\ &= -[y_{n-1}, y_{n-2}, ..., y_{n-p}] \begin{bmatrix} a_{n1} \\ a_{n2} \\ \vdots \\ a_{np} \end{bmatrix} + v_n, \end{aligned} \tag{9}$$

where v_n is the input white noise and the $a_{ni} (i = 1, ..., p)$ coefficients are the p time-varying AR parameters at the time-instance of n. So by defining $\mathbf{x}_n = [a_{n1}, a_{n2}, ..., a_{np}]^T$ as a state vector, and $\mathbf{h}_n = -[y_{n-1}, y_{n-2}, ..., y_{n-p}]^T$, we can reformulate the problem of AR parameter estimation in the KF form as follows:

$$\begin{cases} \mathbf{x}_{n+1} = \mathbf{x}_n + \mathbf{w}_n \\ y_n = \mathbf{h}_n^T \mathbf{x}_n + v_n, \end{cases} \tag{10}$$

where we have assumed that the temporal evolution of the time-varying AR parameters follows a random walk model with a white Gaussian input noise vector $\mathbf{w}_n$. This approach is a conventional and practical assumption in the KF context when there is no *a priori* information about the dynamics of a state vector [36].

To solve the standard KF equations [36], we also require the expected initial state vector $\bar{\mathbf{x}}_0 = E\{\mathbf{x}_0\}$, its covariance matrix $P_0 = E\{\bar{\mathbf{x}}_0 \bar{\mathbf{x}}_0^T\}$, the covariance matrices of the Process noise $Q_n = E\{\mathbf{w}_n \mathbf{w}_n^T\}$, and the measurement noise variance $r_n = E\{v_n v_n^T\}$.

$\bar{\mathbf{x}}_0$ can be estimated from a global (time-invariant) AR model fitting over the whole samples of y_n, and its covariance matrix (P_0) can be selected large enough to indicate the imprecision of the initial estimate. The effects of these initial states are of less importance and usually vanish in time, under some general convergence properties of KFs.

By considering the AR parameters to be uncorrelated, the covariance matrix of Q_n can be selected as a diagonal matrix. The selection of the entries of this matrix, depends on the extent of y_n's non-stationarity. For quasi-stationary noises, the diagonal entries of Q_n are rather small, while for highly non-stationary noises they are large. Generally the selection of this matrix is a compromise between convergence rate and stability. Finally, r_n is selected according to the desired variance of the output noise.

To complete the discussion, the AR model order should also be selected. It is known that for stationary AR models, there are information-based criteria such as the *Akaike Information Criterion* (AIC) for the selection of the optimal model order. However, for time-varying models the selection is not as straightforward since the model is dynamically evolving in time. In general, the model order should be less than the optimal order of a global time-invariant model. For example, in this study an AR order of twelve to sixteen was found to be sufficient for a time-invariant AR model of BW noise, using the AIC. Based on this, the order of the time-variant AR model was selected to be twelve, which led to the generation of realistic noise samples.

Now having the time-varying AR model, it is possible to generate noises with different variances. As an illustration, in Fig. 5 a one minute long segment of BW with a sampling rate of 360Hz, taken from the NSTDB [34], [38], and the synthetic BW noise generated by the proposed method are depicted. The frequency response magnitude of the time-varying AR filter designed for this BW noise is depicted in Fig. 6. As it can be seen, the time-varying AR model is acting as an adaptive filter which is adapting its frequency response to the contents of the non-stationary noise.

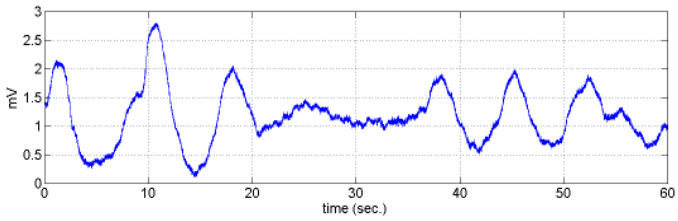

(a)

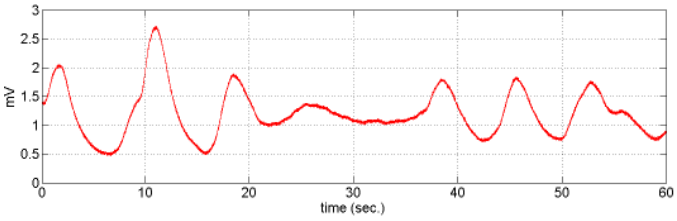

(b)

Fig. 5. Typical segment of ECG BW Noise (a) Original (b) Synthetic

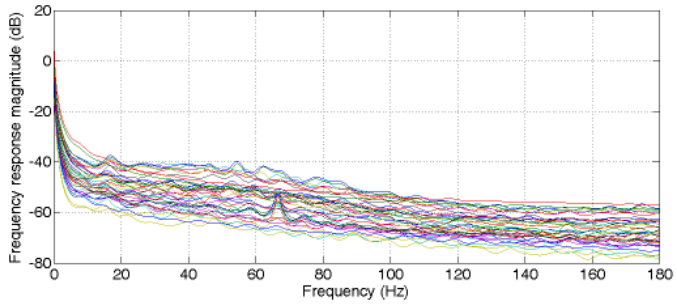

Fig. 6. Frequency response magnitudes of 32 segments of the time-varying AR filters for the Baseline Wander noises of the NSTDB. This figure illustrates how the AR filter responses are evolving in time.

It should be noted that since the vector $\mathbf{h}_n$ varies with time, it is very important to monitor the covariance matrix of the KF's error and the innovation signal, to be sure about the stability and fidelity of the filter.

By using the KF framework it is also possible to monitor the stationarity of the y_n signals, and to update the AR parameters as they tend to become non-stationary. For this, the variance of the innovation signal should be monitored, and the KF state vectors (or the AR parameters) be updated only whenever the variance of the innovation increases beyond a predefined value. There have also been some ad hock methods developed, for updating the covariance matrices of the observation and process noises and to prevent the divergence of the KF [37].

For the studies in which a continuous measure of the noise color effect is requires, the spectral shape of the output noise can also be altered by manipulating the poles of the time-varying AR model over the unit circle, which is identical to *warping* the frequency axis of the AR filter response [39].

V. Results

The approach presented in this work for generating synthetic ECG signals is believed to have interesting applications from both the theoretical and practical point of view. Here we shall study the accuracy of the synthetic model and a special case study.

TABLE II

The percentage of MSE in the synthetic VCG channels using five and nine Gaussian functions

VCG Channel	5 Gaussians	9 Gaussians
V_x	1.24	0.09
V_y	1.68	0.15
V_z	3.60	0.12

A. The model accuracy

In this example, the model accuracy will be studied for a typical ECG signal of the Physikalisch-Technische Bundesanstalt Diagnostic ECG Database (PTBDB) [40], [41], [42]. The database consists of the standard twelve channel ECG recordings and the three Frank lead VCGs. In order to have a clean template for extracting the model parameters, the signals are pre-processed by a band-pass filter to remove the baseline wander and high frequency noises. The ensemble average of the ECG is then extracted from each channel. Next, the parameters of the Gaussian functions of the synthetic model are extracted from the ensemble average of the Frank lead VCGs by using the nonlinear least squares procedure explained in section III-C. The Original VCGs and the synthetic ones generated by using five and nine Gaussian functions are depicted in Figs. 7(a)–7(c) for comparison. The *mean square error* (MSE) of the two synthetic VCGs with respect to the true VCGs are listed in Table II.

The H matrix defined in (5) may also be calculated by solving the MMSE transformation between the ECG and the three VCG channels (similar to (8)). As with the Dower transform, H can be used to find approximative ECGs from the three original VCGs or the synthetic VCGs. In Figs. 7(d)–7(f), the original ECGs of channels V_1, V_2, and V_6, and the approximative ones calculated from the VCG are compared with the ECGs calculated from the synthetic VCG using five and nine Gaussian functions for one ECG cycle. As it can be seen in these results, the ECGs which are reconstructed from the synthetic VCG model have significantly improved as the number of Gaussian functions have been increased from five to nine, and the resultant signals very well resemble the ECGs which have been reconstructed from the original VCG by using the Dower transform. The model improvement is especially notable, around the asymmetric segments of the ECG such as the T-wave.

However, it should be noted that the ECG signals which are reconstructed by using the Dower transform (either from the original VCG or the synthetic ones), do not perfectly match the true recorded ECGs, especially in the low amplitude segments such as the P-wave. This in fact shows the intrinsic limitation of the single dipole model in representing the low-amplitude components of the ECG which require more than three dimensions for their accurate representation [11]. The MSE of the calculated ECGs of Figs. 7(d)–7(f) with respect to the true ECGs are listed in Table III.

B. Fetal ECG extraction

We will now present an application of the proposed model for evaluating the results of source separation algorithms.

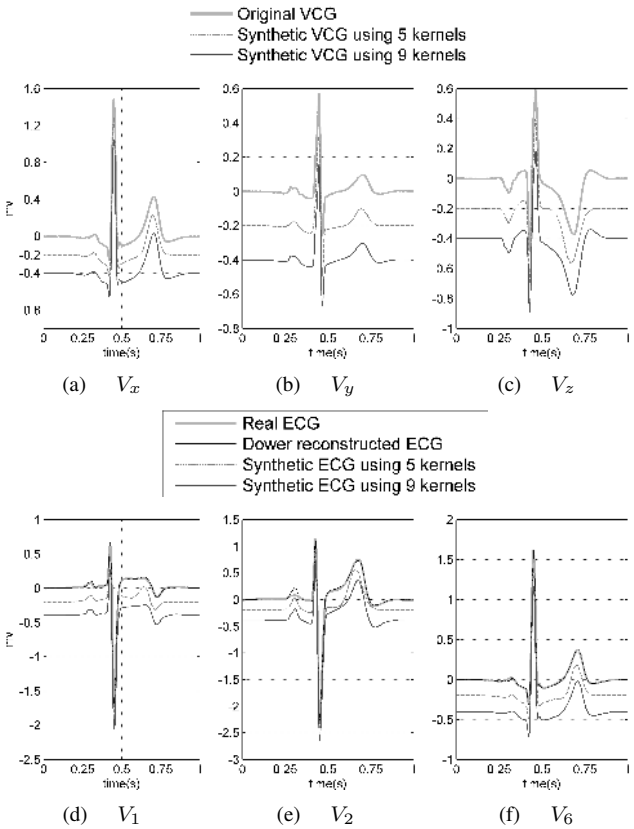

Fig. 7. Original vs. synthetic VCGs and ECGs using 5 and 9 Gaussian functions. For comparison, the ECG reconstructed from the Dower transformation is also depicted in (d)-(f) over the original ECGs. The synthetic VCGs and ECGs have been vertically shifted 0.2mV for better comparison. Refer to text for details.

TABLE III

THE PERCENTAGE OF MSE IN THE ECGS RECONSTRUCTED BY DOWER TRANSFORMATION FROM THE ORIGINAL VCG AND FROM THE SYNTHETIC VCG USING FIVE AND NINE GAUSSIAN FUNCTIONS

ECG Channel	Original VCG	5 Gaussians	9 Gaussians
V_1	0.78	2.06	0.86
V_2	0.67	3.14	0.72
V_6	0.16	1.12	0.19

To generate synthetic maternal abdominal recordings, consider two dipole vectors for the mother and the fetus as defined in (4). The dipole vector of the mother is assumed to have the parameters listed in Table I with a heart rate of $f_m = 0.9$Hz, and the fetal dipole is assumed to have the parameters listed in Table IV, with a heart beat of $f_f = 2.2$Hz. As seen in Table IV, the amplitudes of the Gaussian terms used for modeling the fetal dipole have been chosen to be an order of magnitude smaller than their maternal counterparts.

Further consider the fetus to be in the normal vertex position shown in Fig. 8, with its head down and its face towards the right arm of the mother. To simulate this position, the angles of R_0 defined in (7) can be selected as follows: $\theta_x = -3\pi/4$ to rotate the fetus around the x axis of the maternal body to place it in the head-down position, $\theta_y = 0$ to indicate no fetal rotation around the y axis, and $\theta_z = -\pi/2$ to rotate the fetus

TABLE IV

PARAMETERS OF THE SYNTHETIC FETAL DIPOLE USED IN SECTION V-B

Index(i)	1	2	3	4	5
α_i^x(mV)	0.007	-0.011	0.13	0.007	0.028
b_i^x(rads.)	0.1	0.03	0.05	0.02	0.3
θ_i(rads.)	-0.7	-0.17	0	0.18	1.4
α_i^y(mV)	0.004	0.03	0.045	-0.035	0.005
b_i^y(rads.)	0.1	0.05	0.03	0.04	0.3
θ_j(rads.)	-0.9	-0.08	0	0.05	1.3
α_i^z(mV)	-0.014	0.003	-0.04	0.046	-0.01
b_i^z(rads.)	0.1	0.4	0.03	0.03	0.3
θ_k(rads.)	-0.8	-0.3	-0.1	0.06	1.35

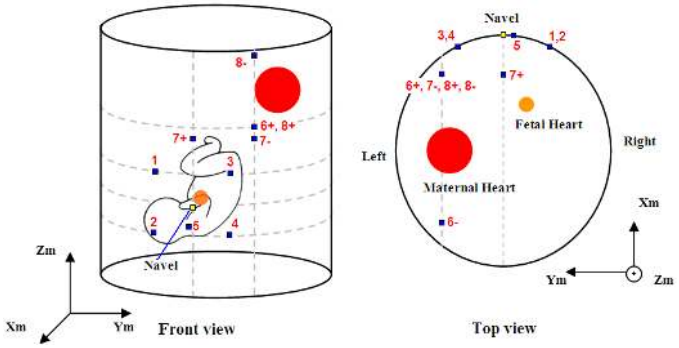

Fig. 8. Model of the maternal torso, with the locations of the maternal and fetal hearts and the simulated electrode configuration

towards the right arm of the mother[1].

Now according to (6), to model maternal abdominal signals, the transformation matrices of H_m and H_f are required, which depend on the maternal and fetal body volume conductor as the propagation medium. As a simplified case consider this volume conductor to be a homogeneous infinite medium which only contains the two dipole sources of the mother and the fetus. Also consider five abdominal electrodes with a reference electrode of the maternal navel, and three thoracic electrode pairs for recording the maternal ECGs, as illustrated in Fig. 8. This electrode configuration is in accordance with real measurement systems presented in [9], [43], [44], in which several electrodes are placed over the maternal abdomen and thorax to record the fECG in any fetal position without changing the electrode configuration. From the source separation point of view, the maximal spatial diversity of the electrodes with respect to the signal sources such as the maternal and fetal hearts is expected to improve the separation performance. The location of the maternal and fetal hearts and the recording electrodes are presented in Table V for a typical shape of a pregnant woman's abdomen. In this table, the maternal navel is considered as the origin of the coordinate system.

Previous studies have shown that low conductivity layers which are formed around the fetus (like the *vernix caseosa*) have great influence on the attenuation of the fetal signals. The conductivity of these layers has been measured to be about 10^6-times smaller than their surrounding tissues; meaning that even a very thin layer of these tissues has considerable effect

[1]The negative signs of θ_x, θ_y, and θ_z are due to the fact that by definition, R_0 is the matrix which transforms the fetal coordinates to the maternal coordinates.

TABLE V

THE SIMULATED ELECTRODE AND HEART LOCATIONS *

	Abdominal leads					Thoracic lead pairs						Heart locations	
Index	1	2	3	4	5	6+	6−	7+	7−	8+	8−	Maternal heart	Fetal heart
x (cm)	-5	-5	-5	-5	-5	-10	-35	-10	-10	-10	-10	-25	-15
y (cm)	-7	-7	7	7	-1	10	10	0	10	10	10	7	-4
z (cm)	7	-7	7	-7	-5	18	18	15	15	18	24	20	2

* The maternal navel is assumed as the center of the coordinate system and the reference electrode for the abdominal leads.

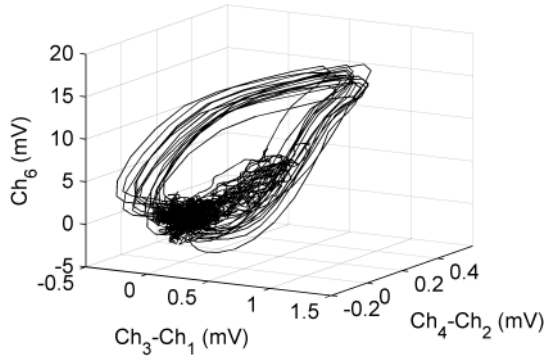

Fig. 9. Synthetic mixture of the maternal and fetal VCGs, using a combination of the leads defined in Table V.

on the fetal components [4]. The complete solution of this problem which encounters the conductivities of different layers of the body tissues requires a much more sophisticated model of the volume conductor, which is beyond the scope of this example. For simplicity we define the constant terms in (3) as $\kappa \doteq \frac{1}{4\pi\sigma}$, and assume $\kappa = 1$ for the maternal dipole and $\kappa = 0.1$ for the fetal dipole. These values of κ lead to simulated signals having maternal to fetal peak-amplitude-ratios, that are in accordance with real abdominal measurements such as the DaISy database [43].

Using (2) and (3), the electrode locations, and the volume conductor conductivities, we can now calculate the coefficients of the transformation between the dipole vector and each of the recording electrodes for both the mother and the fetus (Table VI).

The next step is to generate realistic ECG noise. For this example a one minute mixture of noises has been produced by summing normalized portions of real baseline wander, muscle artifacts, and electrode movement noises of the NSTDB [38], [34]. The time-varying AR coefficient described in section IV, may be calculated for this mixture. We can now generate different instances of synthetic ECG noise by using different instances of white noise as the input of the time-varying AR model. Normalized portions of these noises can be added to the synthetic ECG to achieve synthetic ECGs with desired SNRs.

A five second segment of eight maternal channels generated with this method can be seen in Fig. 10. In this example, the SNR of each channel is 10dB. Also as an illustration, the 3-D VCG loop constructed from a combination of three pairs of the electrodes are depicted in Fig. 9.

As previously mentioned, the multi-channel synthetic recordings described in this article can be used to study the performance of the signal processing tools previously developed for ECG analysis. As a typical example, the JADE ICA algorithm [45] was applied to the eight synthetic channels to extract eight independent components. The resultant Independent Components (ICs) can be seen in Fig. 11.

According to these results, three of the extracted ICs correspond to the maternal ECG, and two with the fetal ECG. The other channels are mainly the noise components, but still contain some element of the fetal R-peaks. Moreover some peaks of the fetal components are still valid in the maternal components, meaning that ICA has failed to completely separate the maternal and fetal components.

To explain these results, we should note that the dipole model presented in (4) has three linearly independent dimensions. This means that if the synthetic signals were noiseless, we could only have six linearly independent channels (three due to the maternal dipole and three due to the fetal), and any additional channel would be a linear combination of the others. However, for noisy signals additional dimensions are introduced which correspond to noise. In the ICA context, it is known that the ICs extracted from noisy recordings can be very sensitive to noise. In this example in particular, the co-planar components of the maternal and fetal subspaces are more sensitive and may be dominated by noise. This explains why the traces of the fetal component are seen among the maternal components, instead of being extracted as an independent component [11]. The quality of the extracted fetal components may be improved by denoising the signals with e.g. wavelet denoising techniques, before applying ICA [10].

This example demonstrates that by using the proposed model for body surface recordings with different source separation algorithms, it is possible to find interesting interpretations and theoretical bases for previously reported empirical results.

VI. DISCUSSIONS AND CONCLUSIONS

In this paper a three dimensional model of the dipole vector of the heart was presented. The model was then used for the generation of synthetic multi-channel signals recorded from the body surface of normal adults and pregnant women. A practical means of generating realistic ECG noises, which are recorded in real conditions, was also developed. The effectiveness of the model, particularly for fetal ECG studies, was illustrated through a simulated example. Considering the simplicity and generality of the proposed model, there are many other issues which may be addressed in future works, some of which will now be described.

TABLE VI

THE CALCULATED MIXING MATRICES FOR THE MATERNAL AND FETAL DIPOLE VECTORS

$$H_m^T = 10^{-3} \times \begin{bmatrix} 0.23 & -0.30 & 0.76 & -0.18 & -0.15 & 12.41 & -0.70 & -0.20 \\ -0.46 & -0.09 & 0.20 & 0.20 & -0.02 & -1.68 & -2.07 & -0.04 \\ -0.05 & 0.01 & -0.39 & -0.14 & -0.13 & 1.12 & 0.23 & -2.21 \end{bmatrix}$$

$$H_f^T = 10^{-3} \times \begin{bmatrix} 0.25 & -0.01 & -0.13 & -0.20 & 0.11 & 0.13 & 0.10 & 0.04 \\ -0.30 & -0.22 & 0.18 & 0.11 & 0.05 & 0.08 & -0.05 & 0.11 \\ 0.37 & -0.29 & 0.18 & -0.12 & -0.30 & 0.09 & 0.26 & 0.05 \end{bmatrix}$$

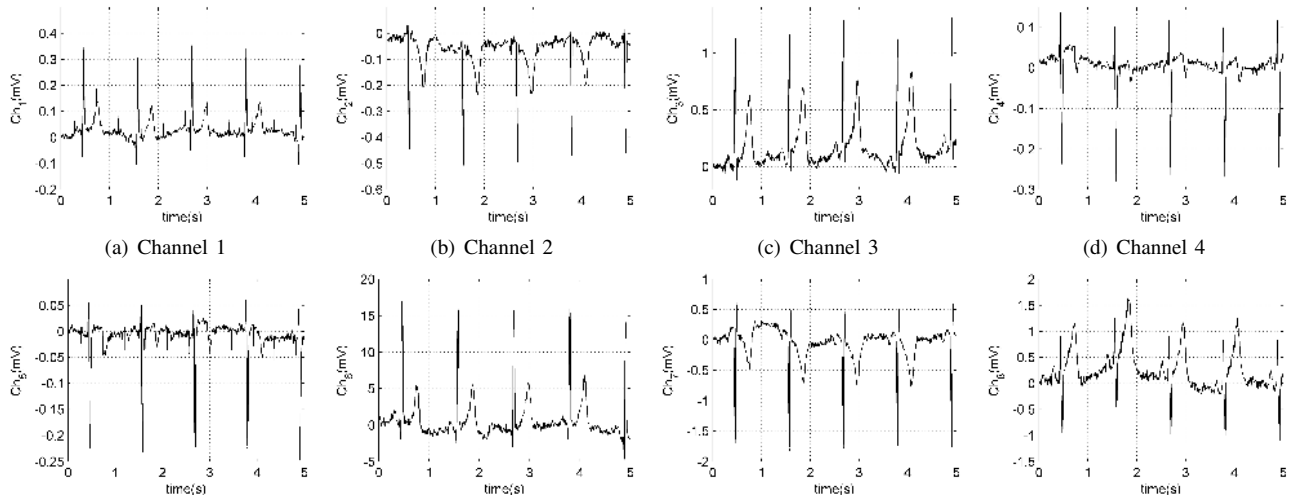

(a) Channel 1 (b) Channel 2 (c) Channel 3 (d) Channel 4

(e) Channel 5 (f) Channel 6 (g) Channel 7 (h) Channel 8

Fig. 10. Synthetic multi-channel signals from the maternal abdomen (channels 1-5) and thorax (channels 6-8). Notice the small fetal components with a frequency almost twice the maternal heart rate in the abdominal channels.

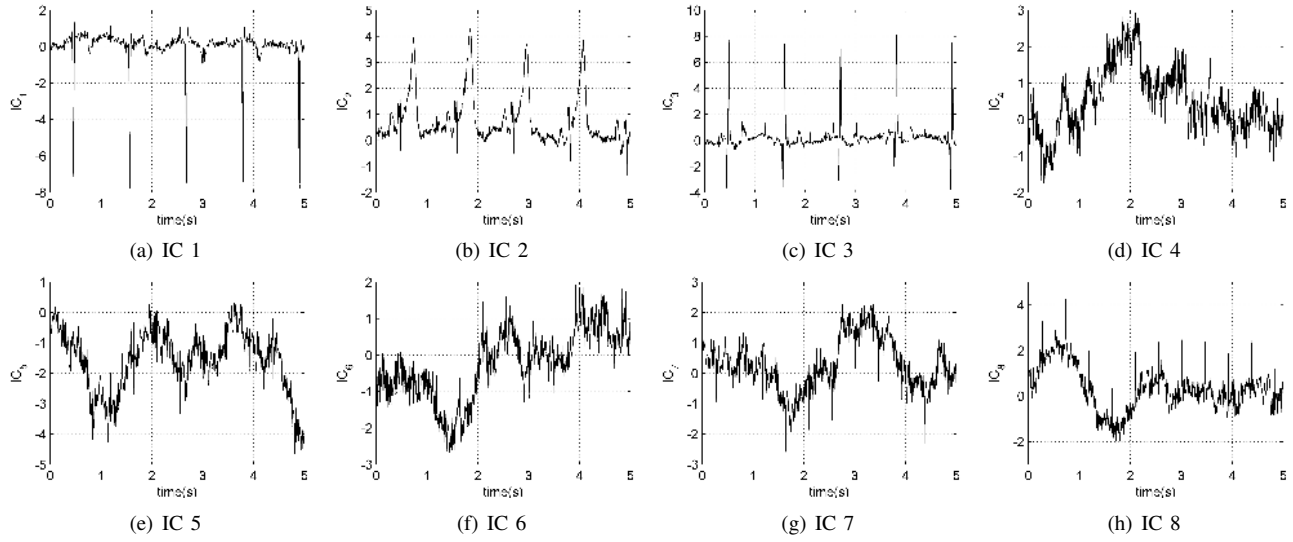

(a) IC 1 (b) IC 2 (c) IC 3 (d) IC 4

(e) IC 5 (f) IC 6 (g) IC 7 (h) IC 8

Fig. 11. Independent Components (ICs) extracted from the synthetic multi-channel recordings. Strong maternal presence can be seen in the first three components. Fetal cardiac activity can be clearly seen in the last three components.

In the presented results, an intrinsic limitation of the single dipole model of the heart was shown. To overcome this limitation, more than three dimensions may be used to represent the cardiac dipole model in (4). In recent works it has been shown that up to five or six dimensions may be necessary for the better representation of the cardiac dipole [11].

In future works, the idea of extending the single dipole model to moving dipoles which have higher accuracies, can also be studied [2]. For such an approach, the dynamic representation in (4) can be very useful. In fact the moving dipole would be simply achieved by adding oscillatory terms to the x, y, and z coordinates in (4), to represent the speed of the heart's dipole movement. In this case, besides the modeling aspect of the proposed approach, it can also be used as a

model-based method of verifying the performance of different heart models.

Looking back to the synthetic dipole model in (4), it is seen that this dynamic model could have also been presented in the direct form (by simply integrating these equations with respect to time). However the state-space representation has the benefit of allowing the study of the evolution of the signal dynamics using state-space approaches [36]. Moreover the combination of (4) and (5) can be effectively used as the basis for Kalman filtering of noisy ECG observations, where (4) represents the underlying dynamics of the noisy recorded channels. In some related works, the authors have developed a nonlinear model-based Bayesian filtering approach (such as the Extended Kalman Filter) for denoising single channel ECG signals [24], [32], [46], which led to superior results compared with conventional denoising techniques. However, the extension of such proposed approaches for multichannel recordings requires the multi-dimensional modeling of the heart dipole vector which is presented in this paper. In fact, multiple ECG recordings can be used as multiple observations for the Kalman filtering procedure, which is believed to further improve the denoising results. The Kalman filtering framework is also believed to be extensible to the filtering and extraction of fetal ECG components. In this case the dynamic evolutions of the fetal and maternal dipoles are modeled with (4), and (6) can be assumed as the observation equation.

Following the discussions in section III, it is known that Gaussian mixtures are capable of modeling any ECG signal, even with asymmetric shapes such as the T-wave (which is rather common in real recordings). However in these cases, two or more Gaussian terms or a *log-normal* function may be required to model the asymmetric shape. For such applications, it could be simpler to substitute the Gaussian functions with naturally asymmetric functions, such as the *Gumbel function* which has a Gaussian shape that is skewed towards the right- or left-side of its peak [47]. A log-normal distribution may give the same results as the Gumbel, but the Gumbel function allows a more intuitive parameterization in terms of the width and hence onsets and offsets in the ECG. This may be useful for determining the end of the T-wave, for example, with a high degree of accuracy.

APPENDIX I
TIME-VARYING VOLUME CONDUCTOR MODELS

As mentioned in section III, the H, R, and Λ matrices are generally functions of time, having oscillations which are coupled with the respiration rate or the heart beat. This oscillatory coupling may be modeled by using the idea of Givens rotation matrices [48].

In terms of geometric rotations, any rotation in the N dimensional space can be decomposed into $L = N(N-1)/2$ rotations corresponding to the number of possible rotation planes in the N dimensional space. This explains why N dimensional rotation matrices, also known as *orthonormal matrices*, have only L degrees of freedom. With this explanation, any orthonormal matrix can be decomposed into L single rotations, as follows:

$$R = \prod_{i=1\ldots N-1, j=i+1\ldots N} R_{ij}, \tag{11}$$

where R_{ij} is the Givens rotation matrix of the i–j plane, derived from an N dimensional identity matrix with the four following changes in its entries:

$$\begin{array}{ll} R_{ij}(i,i) = cos(\theta_{ij}), & R_{ij}(i,j) = sin(\theta_{ij}) \\ R_{ij}(j,i) = -sin(\theta_{ij}), & R_{ij}(j,j) = cos(\theta_{ij}), \end{array} \tag{12}$$

and θ_{ij} is the rotation angle between the i and j axes, in the i–j plane. The R_0 matrix presented in (7) is a 3-dimensional example of the general rotation in (11).

Now in order to achieve a time-varying rotation matrix which is coupled with an external source, such as the respiration rate or heart beat (either of the adult or the fetus), any of the θ_{ij} rotation angles can oscillate with the external source frequency, as follows:

$$\theta_{ij}(t) = \theta_{ij}^{max} sin(2\pi f t) \tag{13}$$

where θ_{ij}^{max} is the maximum deviation of the θ_{ij} rotation angle, and f is the frequency of the external source. The axes which are coupled with the oscillatory source, depend on the nature of the sources of interest and the geometry of the problem (i.e. the relative location and distance of the sources), and apparently depending on this geometry other means of coupling are also possible.

The presented time-varying rotation matrices can be used to model the rotation matrices of the synthetic ECG models defined in (5) and (6), or as multiplicative factors for the H matrices in these equations.

ACKNOWLEDGMENT

The authors would like to acknowledge the support of the Iranian-French scientific cooperation program (PAI Gundishapur) and the National Institute of Biomedical Imaging and Bioengineering under Grant Number R01 EB001659.

REFERENCES

[1] O. Dössel, "Inverse problem of electro- and magnetocardiography: Review and recent progress," *Int. J. Bioelectromagnetism*, vol. 2, no. 2, 2000. [Online]. Available: http://www.ijbem.org/volume2/number2/doessel/paper.htm

[2] A. van Oosterom, "Beyond the dipole; modeling the genesis of the electrocardiogram," *100 years Einthoven*, pp. 7–15, 2002, the Einthoven Foundation, Leiden.

[3] J. A. Malmivuo and R. Plonsey, Eds., *Bioelectromagnetism, Principles and Applications of Bioelectric and Biomagnetic Fields*. Oxford University Press, 1995. [Online]. Available: http://butler.cc.tut.fi/~malmivuo/bem/bembook

[4] T. Oostendorp, *Modeling the Fetal ECG*. Ph.D. dissertation, K. U. Nijmegen, The Netherlands, 1989.

[5] P. P. Kanjilal, S. Palit, and G. Saha, "Fetal ECG extraction from single-channel maternal ECG using singular value decomposition," *IEEE Trans. Biomed. Eng.*, vol. 44, pp. 51–59, Jan. 1997.

[6] P. Gao, E.-C. Chang, and L. Wyse, "Blind Separation of Fetal ECG from Single Mixture using SVD and ICA," in *Proceedings of ICICS-PCM 2003*, December 2003, pp. 1418–1422.

[7] D. Callaerts, W. Sansen, J. Vandewalle, G. Vantrappen, and J. Janssens, "Description of a real-time system to extract the fetal electrocardiogram," *Clinical Physics and Physiological Measurement*, vol. 10, no. 4B, pp. 7–10, 1989. [Online]. Available: http://stacks.iop.org/0143-0815/10/7

[8] L. de Lathauwer, B. de Moor, and J. Vandewalle, "Fetal electrocardiogram extraction by blind source subspace separation," *IEEE Trans. Biomed. Eng.*, vol. 47, pp. 567–572, May 2000.

[9] F. Vrins, C. Jutten, and M. Verleysen, "Sensor array and electrode selection for non-invasive fetal electrocardiogram extraction by independent component analysis," in *Independent Componenent Analysis and Blind Signal Separation*, ser. Lecture Notes in Computer Science (LNCS 3195), A. P. C.G. Puntonet, Ed. Springer, 2004, pp. 1017–1024.

[10] B. Azzerboni, F. La Foresta, N. Mammone, and F. C. Morabito, "A new approach based on wavelet-ica algorithms for fetal electrocardiogram extraction." in *Proceedings of the 13th European Symposium on Artificial Neural Networks (ESANN 2005)*, 2005, pp. 193–198.

[11] R. Sameni, C. Jutten, and M. B. Shamsollahi, "What ICA Provides for ECG Processing: Application to Noninvasive Fetal ECG Extraction," in *Proc. of the International Symposium on Signal Processing and Information Technology (ISSPIT'06)*, Vancouver, Canada, August 2006, pp. 656–661.

[12] A. Cichocki and S. Amari, Eds., *Adaptive Blind Signal and Image Processing*. John Wiley & Sons Inc., 2003.

[13] P. E. McSharry, G. D. Clifford, L. Tarassenko, and L. A. Smith, "A Dynamic Model for Generating Synthetic Electrocardiogram Signals," *IEEE Trans. Biomed. Eng.*, vol. 50, pp. 289–294, mar 2003.

[14] P. E. McSharry and G. D. Clifford, *ECGSYN - A realistic ECG waveform generator*. [Online]. Available: http://www.physionet.org/physiotools/ecgsyn/

[15] P. Bergveld and W. J. H. Meijer, "A New Technique for the Supression of the MECG," *IEEE Trans. Biomed. Eng.*, vol. BME-28, pp. 348–354, Apr. 1981.

[16] W. J. H. Meijer and P. Bergveld, "The Simulation of the Abdominal MECG," *IEEE Trans. Biomed. Eng.*, vol. BME-28, pp. 354–357, Apr. 1981.

[17] D. B. Geselowitz, "On the Theory of the Electrocardiogram," *Proc. IEEE*, vol. 77, pp. 857–876, Jun. 1989.

[18] E. Frank, "An Accurate, Clinically Practical System For Spatial Vectorcardiography," *Circulation*, vol. 13, no. 5, pp. 737–749, 1956. [Online]. Available: http://circ.ahajournals.org/cgi/content/abstract/13/5/737

[19] G. F. Fletcher, G. Balady, V. F. Froelicher, L. H. Hartley, W. L. Haskell, and M. L. Pollock, "Exercise Standards : A Statement for Healthcare Professionals From the American Heart Association," *Circulation*, vol. 91, no. 2, pp. 580–615, 2001. [Online]. Available: http://circ.ahajournals.org

[20] G. E. Dower, H. B. Machado, and J. A. Osborne, "On deriving the electrocardiogram from vectorcardiographic leads," *Clin. Cardiol.*, vol. 3, p. 87, 1980.

[21] L. Hadzievski, B. Bojovic, V. Vukcevic, P. Belicev, S. Pavlovic, Z. Vasiljevic-Pokrajcic, and M. Ostojic, "A novel mobile transtelephonic system with synthesized 12-lead ECG," *IEEE Trans. Inform. Technol. Biomed.*, vol. 8, pp. 428–438, Dec. 2004.

[22] L. Edenbrandt and O. Pahlm, "Vectorcardiogram synthesized from a 12-lead ECG: Superiority of the inverse Dower matrix," *J. Electrocardiol.*, vol. 21, p. 361, 1988.

[23] G. D. Clifford and P. E. McSharry, "A realistic coupled nonlinear artificial ECG, BP, and respiratory signal generator for assessing noise performance of biomedical signal processing algorithms," *Proc of SPIE International Symposium on Fluctuations and Noise*, vol. 5467, no. 34, pp. 290–301, 2004.

[24] R. Sameni, M. B. Shamsollahi, C. Jutten, and M. Babaie-Zadeh, "Filtering Noisy ECG Signals Using the Extended Kalman Filter Based on a Modified Dynamic ECG Model," in *Proceedings of the 32nd Annual International Conference on Computers in Cardiology*, Lyon, France, September 25-28 2005, pp. 1017–1020.

[25] G. Clifford, "A novel framework for signal representation and source separation," *Journal of Biological Systems*, vol. 14, no. 2, pp. 169–183, June 2006.

[26] J. Ben-Arie and K. Rao, "Nonorthogonal representation of signals by Gaussians and Gabor functions," *IEEE Trans. Circuits Syst. II*, vol. 42, no. 6, pp. 402–413, June 1995.

[27] *Fetal Positions, WebMD Inc.* [Online]. Available: http://www.webmd.com/content/tools/1/slide_fetal_pos.htm

[28] G. D. Clifford, A. Shoeb, P. E. McSharry, and B. A. Janz, "Model-based filtering, compression and classification of the ECG," *International Journal of Bioelectromagnetism*, vol. 7, no. 1, pp. 158–161, May 2005.

[29] C. Bishop, *Neural Networks for Pattern Recognition*. New York: Oxford University Press, 1995.

[30] L. Weixue and X. Ling, "Computer simulation of epicardial potentials using a heart-torso model with realistic geometry," *IEEE Trans. Biomed. Eng.*, vol. 43, pp. 211–217, Feb. 1996.

[31] L. Frenkel and M. Feder, "Recursive Expectation-Maximization (EM) Algorithms for Time-varying Parameters with Applications to Multiple Target Tracking," *IEEE Transactions on Signal Processing*, vol. 47, pp. 306–320, Feb. 1999.

[32] R. Sameni, M. B. Shamsollahi, C. Jutten, and G. D. Clifford, "A Nonlinear Bayesian Filtering Framework for ECG Denoising," February 2006, submitted to the IEEE Trans. on Biomed. Eng.

[33] G. M. Friesen, T. C. Jannett, M. A. Jadallah, S. L. Yates, S. R. Quint, and H. T. Nagle, "A comparison of the noise sensitivity of nine QRS detection algorithms," *IEEE Trans. Biomed. Eng.*, vol. 37, no. 1, pp. 85–98, 1990.

[34] G. Moody, W. Muldrow, and R. Mark, "A noise stress test for arrhythmia detectors," in *Computers in Cardiology*, 1984, pp. 381–384.

[35] X. Hu and V. Nenov, "A single-lead ECG enhancement algorithm using a regularized data-driven filter," *IEEE Trans. Biomed. Eng.*, vol. 53, pp. 347–351, Feb. 2006.

[36] A. Gelb, Ed., *Applied Optimal Estimation*. MIT Press, 1974.

[37] M. P. Tarvainen, S. D. Georgiadis, P. O. Ranta-aho, and P. A. Karjalainen, "Time-varying analysis of heart rate variability signals with a Kalman smoother algorithm," *Physiol. Meas.*, vol. 27, pp. 225–239, Mar. 2006.

[38] G. Moody, W. Muldrow, and R. Mark, "The MIT-BIH Noise Stress Test Database," http://www.physionet.org/physiobank/database/nstdb/.

[39] A. Härmä, *Frequency-warped autoregressive modeling and filtering*. Helsinki University of Technology, Espoo, Finland, 2001. [Online]. Available: http://lib.tkk.fi/Diss/2001/isbn9512254603/

[40] *The MIT-BIH PTB Diagnosis Database*. [Online]. Available: http://www.physionet.org/physiobank/database/ptbdb/

[41] R. Bousseljot, D. Kreiseler, and A. Schnabel, "Nutzung der ekg-signaldatenbank cardiodat der ptb uber das internet," *Biomedizinische Technik*, vol. 40, no. 1, pp. S317–S318, 1995.

[42] D. Kreiseler and R. Bousseljot, "Automatisierte ekg-auswertung mit hilfe der ekg-signaldatenbank cardiodat der ptb," *Biomedizinische Technik*, vol. 40, no. 1, pp. S319–S320, 1995.

[43] B. D. Moor, *Database for the Identification of Systems (DaISy)*. [Online]. Available: http://homes.esat.kuleuven.be/~smc/daisy/

[44] M. J. O. Taylor, M. J. Smith, M. Thomas, A. R. Green, F. Cheng, S. Oseku-Afful, L. Y. Wee, N. M. Fisk, and H. M. Gardiner, "Non-invasive fetal electrocardiography in singleton and multiple pregnancies," *BJOG: an International Journal of Obstetrics and Gynaecology*, vol. 110, pp. 668–678, Jul. 2003.

[45] J.-F. Cardoso, *Blind Source Separation and Independent Component Analysis*. [Online]. Available: http://www.tsi.enst.fr/~cardoso/guidesepsou.html

[46] R. Sameni, M. B. Shamsollahi, and C. Jutten, "Filtering Electrocardiogram Signals Using the Extended Kalman Filter," in *Proceedings of the 27th Annual International Conference of the IEEE Engineering in Medicine and Biology Society (EMBS)*, Shanghai, China, September 1-4 2005, pp. 5639–5642.

[47] E. J. Gumbel, *Statistics of Extremes*. Columbia University Press, 1958.

[48] G. Golub and C. van Loan, *Matrix Computations*, 3rd ed. The Johns Hopkins University Press, 1996.